7950 *J. Med. Chem.* **2009,** *52,* 7950–7953
DOI: 10.1021/jm901543m

Journal of Medicinal Chemistry Letter

Discovery of a 2,4-Diamino-7-aminoalkoxyquinazoline as a Potent and Selective Inhibitor of Histone Lysine Methyltransferase G9a[†]

Feng Liu,[‡] Xin Chen,[‡] Abdellah Allali-Hassani,[§] Amy M. Quinn,[∥] Gregory A. Wasney,[§] Aiping Dong,[§] Dalia Barsyte,[§] Ivona Kozieradzki,[§] Guillermo Senisterra,[§] Irene Chau,[§] Alena Siarheyeva,[§] Dmitri B. Kireev,[‡] Ajit Jadhav,[∥] J. Martin Herold,[‡] Stephen V. Frye,[‡] Cheryl H. Arrowsmith,[§] Peter J. Brown,[§] Anton Simeonov,[∥] Masoud Vedadi,[§] and Jian Jin*[,‡]

[‡]*Center for Integrated Chemical Biology and Drug Discovery, Division of Medicinal Chemistry and Natural Products, Eshelman School of Pharmacy, University of North Carolina at Chapel Hill, Chapel Hill, North Carolina 27599,* [§]*Structural Genomics Consortium, University of Toronto, Toronto, Ontario, M5G 1L6, Canada, and* [∥]*NIH Chemical Genomics Center, National Human Genome Research Institute, National Institutes of Health, Bethesda, Maryland 20892*

Received October 18, 2009

Abstract: SAR exploration of the 2,4-diamino-6,7-dimethoxyquinazoline template led to the discovery of **8** (UNC0224) as a potent and selective G9a inhibitor. A high resolution X-ray crystal structure of the G9a−**8** complex, the first cocrystal structure of G9a with a small molecule inhibitor, was obtained. The cocrystal structure validated our binding hypothesis and will enable structure-based design of novel inhibitors. **8** is a useful tool for investigating the biology of G9a and its roles in chromatin remodeling.

Multicellular organisms have evolved elaborate mechanisms to enable differential and cell-type specific expression of genes. Epigenetics refers to these heritable changes in how the genome is accessed in different cell types and during development and differentiation. This capability permits specialization of function between cells even though each cell contains the same genome. Over the past decade, the cellular machinery that creates these heritable changes has been the subject of intense scientific investigation, as there is no area of biology, or for that matter no area of human health, where epigenetics may not play a fundamental role.[1]

The template upon which the epigenome is written is chromatin, the complex of histone proteins, RNA, and DNA that efficiently package the genome in an appropriately accessible state within each cell. The state of chromatin, and therefore access to the genetic code, is mainly regulated by covalent and reversible PTMs[a] to histone proteins and DNA and by the recognition of these marks by other proteins and protein complexes. The PTMs of histones and DNA include histone lysine methylation, arginine methylation, lysine acetylation, sumoylation, ADP-ribosylation, ubiquitination, glycosylation and phosphorylation, and DNA methylation.[2] Given the widespread importance of chromatin regulation to cell biology, the enzymes that produce these modifications (the "writers"), the proteins that recognize them (the "readers"), and the enzymes that remove them (the "erasers") are critical targets for manipulation to further understand the histone code[3,4] and its role in human disease. Indeed, small molecule histone deacetylase inhibitors[5] and DNA methyltransferase inhibitors[6] have already proven useful in the treatment of cancer.

Histone lysine methylation refers to covalent methylation of histone lysine tails to produce mono-, di-, or trimethylated states. Among a myriad of PTMs, histone lysine methylation catalyzed by histone lysine methyltransferases (HMTs) has received great attention because of its essential function in many biological processes including gene expression and transcriptional regulation, heterochromatin formation, and X-chromosome inactivation.[7] It is therefore considered to be one of the most significant PTMs of histones. Since the first HMT was characterized in 2000,[8] more than 50 human histone methyltransferases have been identified.[9] Growing evidence suggests that HMTs play important roles in the development of various human diseases including cancer.[10,11] For example, G9a, a H3K9 methyltransferase also known as EHMT2, is overexpressed in human cancers and knockdown of G9a inhibits cancer cell growth.[12,13]

Despite the tremendous progress made in identifying new HMTs, only two small molecule HMT inhibitors,[14−16] which are not SAM-related analogues, have been reported since the first HMT was characterized in 2000.[8] Therefore, creating multiple, high quality small molecule HMT inhibitors as research tools for studying the biological function of HMTs is urgently needed.

In this Letter, we report the design and synthesis of novel compounds to explore the 2,4-diamino-6,7-dimethoxyquinazoline template, and biological evaluation of these compounds that led to the discovery of **8** (UNC0224) as a potent and selective G9a inhibitor. In addition, we disclose a high resolution (1.7 Å) X-ray crystal structure of the G9a−**8** complex, the first cocrystal structure of G9a with a small molecule inhibitor.

The only previously reported small molecule inhibitor of G9a in the literature is 2,4-diamino-6,7-dimethoxyquinazoline **2a** (BIX-01294)[15,17] (Figure 1), which also inhibited GLP

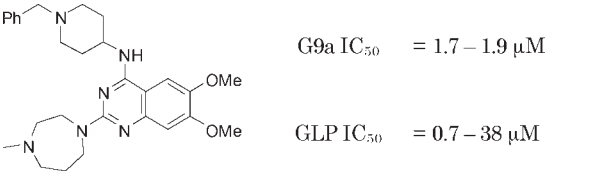

Figure 1. Structure and reported IC_{50} of **2a** against G9a and GLP.[15,17]

[†]The coordinates and structure factors of UNC0224 cocrystallized with G9a have been deposited in the Protein Data Bank (www.pdb.org, PDB code 3K5K).

*To whom correspondence should be addressed. Phone: 919-843-8459. Fax: 919-843-8465. E-mail: jianjin@unc.edu.

[a]Abbreviations: PTMs, post-translational modifications; HMT, histone lysine methyltransferase; EHMT2, euchromatic histone lysine methyltransferase 2; H3K9, histone 3 lysine 9; SAM, *S*-adenosyl-L-methionine; SAR, structure−activity relationship; GLP, G9a-like protein; EHMT1, euchromatic histone lysine methyltransferase 1; SET, suppressor of variegation 3-9, enhancer of zeste, and trithorax; SAH, *S*-adenosyl-L-homocysteine; AlphaScreen, amplified luminescence proximity homogeneous assay; ITC, isothermal titration calorimetry; FP, fluorescence polarization; DSF, differential scanning fluorimetry.

 Published on Web 11/05/2009

Scheme 1. Synthesis of 2,4-Diamino-6,7-dimethoxyquinazolines **2**[a]

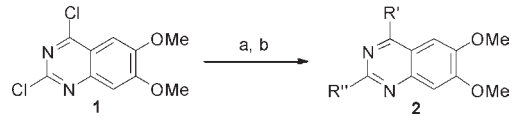

[a](a) R′ amines, DMF, DIEA, room temp; (b) R″ amines, *i*-PrOH, 4 M HCl/dioxane, microwave, 160 °C.

Table 1. SAR of 4-Amino Moiety

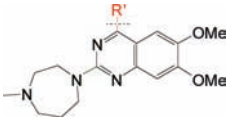

Compound ID	R'	G9a IC$_{50}$ (μM) Thioglo Assay	G9a IC$_{50}$ (μM) Alpha-Screen
2a (BIX-01294)	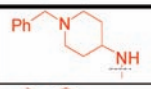	0.11	0.29
2b	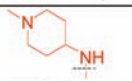	0.33	0.23
2c	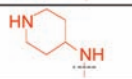	< 30% inhibition at 1 μM	> 10
2d	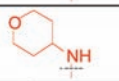	< 30% inhibition at 1 μM	> 10
2e	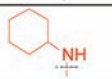	< 30% inhibition at 1 μM	> 10
2f	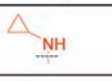	< 30% inhibition at 1 μM	5.1
2g	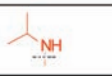	< 30% inhibition at 1 μM	5.8

(also known as EHMT1). GLP is another H3K9 methyltransferase that shares 80% sequence identity with G9a in their respective SET domains. Because no SAR has been reported for this quinazoline scaffold, we decided to explore multiple regions of this template to elucidate the SAR and improve potency and selectivity as part of our efforts to create multiple chemical probes for epigenetic targets and make these probes available to the research community without restrictions on their use.

An efficient two-step synthetic sequence was developed to explore the 4-amino and 2-amino regions of the quinazoline scaffold (Scheme 1). Displacing the 4-chloro of commercially available 2,4-dichloro-6,7-dimethoxyquinazoline (**1**) with the first set of amines at room temperature, followed by displacement of the 2-chloro with the second set of amines under microwave heating conditions, yielded the desired 2,4-diamino-6,7-dimethoxyquinazolines **2** in good yields. Using this efficient synthesis, we rapidly prepared the compounds listed in Tables 1 and 2. These compounds were evaluated in two orthogonal and complementary biochemical assays:[18] (1) ThioGlo-based G9a inhibitory assay for monitoring the conversion of SAM to SAH;[19] (2) G9a AlphaScreen for the detection of methylated histone peptides.[20]

The 4-amino moiety of the quinazoline scaffold was first explored (Table 1). Replacing the 1-benzylpiperidin-4-ylamino group (**2a**) with 1-methylpiperidin-4-ylamino (**2b**) resulted in no potency loss. This result is consistent with the X-ray crystal structure of the GLP−**2a** complex, as the benzyl group of **2a** was outside the peptide binding groove and did not make any interactions.[17] This key SAR finding allowed us to reduce the molecular weight and lipophilicity of this chemical series. On the other hand, replacing the 1-methylpiperidin-4-ylamino (**2b**) with piperidin-4-ylamino (**2c**), tetrahydropyran-4-ylamino (**2d**), or cyclohexylamino (**2e**) led to significant potency loss, indicating that an alkylated nitrogen is important for inhibitory activity. Analogues containing a smaller amino group such as cyclopropylamino (**2f**) and isopropylamino (**2g**) were also significantly less potent compared to **2a** and **2b**. In general, assay results from the ThioGlo-based assay and AlphaScreen are consistent. However, the AlphaScreen appears to be more sensitive for weakly active compounds. The sensitivity of AlphaScreen for weakly active compounds is likely due to the assay detecting amplified signal and to the use of a lower concentration of peptide substrate.

Table 2. SAR of 2-Amino Moiety

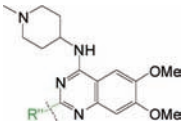

Compound ID	R''	G9a IC$_{50}$ (μM) Thioglo Assay	G9a IC$_{50}$ (μM) Alpha-Screen
2b	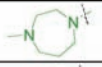	0.33	0.23
2h	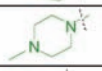	0.68	0.20
2i		0.55	0.51
2j		1.6	0.81
2k		0.91	6.5
2l		1.1	0.90
2m	Cl	< 30% inhibition at 1 μM	9.1

The 2-amino moiety of the quinazoline scaffold was investigated next. In general, modifications to the 2-amino region were well tolerated (Table 2). The methylhomopiperazine (**2b**) could be replaced with the methylpiperazine (**2h**) and piperidine (**2i**) without significant potency loss. Analogues containing morpholine (**2j**), diethylamine (**2k**), or dimethylamine (**2l**) had moderate potency. The 2-chloro analogue **2m** had poor potency in both assays.

Having established initial SAR for the 2- and 4-amino regions, we next explored the 7-methoxy moiety. The X-ray crystal structure of the GLP−**2a** complex revealed that **2a** occupied the histone peptide binding site and did not interact with the narrow lysine binding channel.[17] We hypothesized that adding a 7-aminoalkoxy side chain to the quinazoline scaffold would make new interactions with the lysine binding channel while the rest of molecule maintained interactions with the peptide binding groove. Thus, we designed **8**, which possesses a 7-dimethylaminopropoxy chain and also combines the best 2- and 4-amino moieties identified previously. Synthesis of **8** is outlined in Scheme 2. Benzyl protection of

Scheme 2. Synthesis of Compound **8**[a]

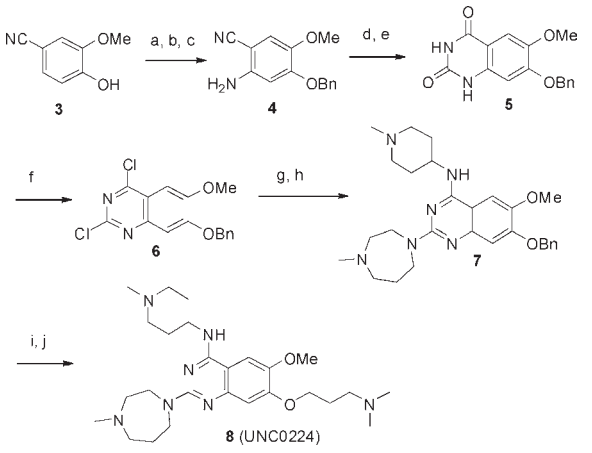

[a] (a) BnBr, K_2CO_3, DMF, room temp; (b) HNO_3, Ac_2O, 0 °C to room temp; (c) Fe dust, NH_4Cl, *i*-PrOH-H_2O, reflux, 67% over 3 steps; (d) methyl chloroformate, DIEA, DMF−DCM, 0 °C to room temp; (e) NaOH, H_2O_2, EtOH, reflux, 70% over 2 steps; (f) *N*,*N*-diethylaniline, $POCl_3$, reflux, 59%; (g) 4-amino-1-methylpiperidine, DIEA, THF, room temp; (h) 1-methylhomopiperazine, HCl, *i*-PrOH, 160 °C, microwave, 82% over 2 steps; (i) Pd/C, H_2, EtOH, room temp; (j) 3-(dimethylamino)propan-1-ol, PPh_3, DIAD, THF, 0 °C to room temp, 46% over 2 steps.

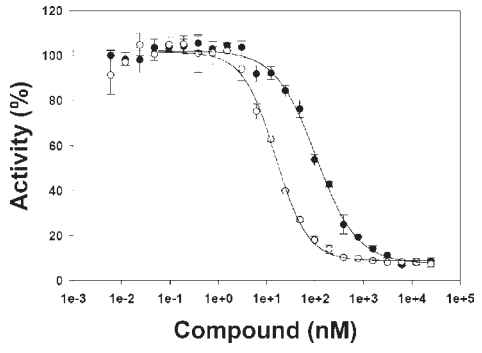

Figure 2. Full concentration response curves of **8** (○) (IC_{50} = 15 ± 10 nM) and **2a** (●) (IC_{50} = 106 ± 20 nM) in the G9a ThioGlo assay.

commercially available 2-methoxy-4-cyanophenol (**3**) followed by nitration and subsequent reduction of the nitro group produced aniline **4**. Aniline **4** was then converted to quinazolinedione **5** via formation of methyl carbamate and subsequent saponification of the cyano group and ring closure. $POCl_3$ treatment of intermediate **5** resulted in 2,4-dichloroquinazoline **6**, which underwent two consecutive chloro displacement reactions to yield 2,4-diaminoquinazoline **7**. Debenzylation of intermediate **7**, followed by Mitsunobu reaction with 3-(dimethylamino)propan-1-ol, produced the desired **8**.

We were pleased to find that **8** was a potent G9a inhibitor with an IC_{50} of 15 nM, 7 times more potent compared to **2a** (IC_{50} = 106 nM), in the G9a ThioGlo assay (Figure 2). Although **8** (IC_{50} = 289 nM) had similar potency compared to **2a** (IC_{50} = 290 nM) in the G9a AlphaScreen (likely due to **8** reaching the IC_{50} limit of the G9a AlphaScreen), the high potency of **8** was confirmed in several secondary assays. In ITC experiments that measure the binding affinity of a small molecule to the G9a protein,[21] **8** (K_d = 23 ± 8 nM (n = 2)) has about 5-fold higher binding affinity compared to **2a** (K_d = 130 ± 18 nM (n = 2)) (Figure 3). **8** also displaced fluorescein

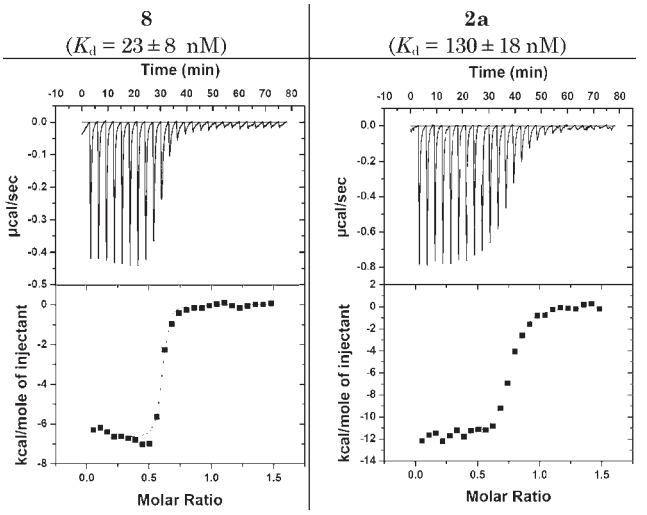

Figure 3. **8** showed higher binding affinity to G9a compared to **2a** in an ITC experiment.

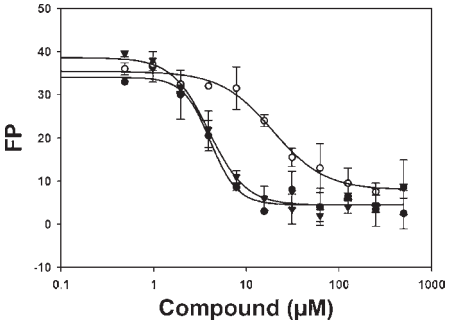

Figure 4. **8** (●) displaced fluorescein labeled 15-mer H3 peptide (1−15) better than **2a** (○) (unlabeled 25-mer H3 peptide (1−25) (▼) used as a positive control).

labeled 15-mer H3 peptide (1−15) better than **2a** in a G9a FP assay (Figure 4). In addition, **8** stabilized G9a better compared to **2a** in DSF experiments.[22] These results together strongly suggest that **8** is a significantly more potent G9a inhibitor compared to **2a**.

Although **8** also potently inhibited GLP with an IC_{50} of 20 and 58 nM in the ThioGlo assay and AlphaScreen, respectively, **8** was more than 1000-fold selective for G9a over SET7/9 (a H3K4 HMT) and SET8/PreSET7 (a H4K20 HMT) in ThioGlo-based biochemical assays. In addition, **8** was clean (less than 20% inhibitions at 1 μM) against a broad range of G-protein-coupled receptors, ion channels, and transporters in a 30-target selectivity panel (tested by MDS Pharma Services) except hitting muscarinic M_2 receptor at 82% inhibition at 1 μM and histamine H_1 receptor at 31% inhibition at 1 μM.

A high resolution (1.7 Å) X-ray crystal structure of the G9a−**8** complex, the first crystal structure of a G9a−small molecule inhibitor complex, was obtained. As shown in Figure 5, we were pleased to find that the 7-dimethylaminopropoxy side chain of **8** indeed occupied the lysine binding channel of G9a nicely, thus validating our binding hypothesis. The higher potency of **8** compared to **2a** can be explained by these additional interactions between the 7-dimethylaminopropoxy side chain and the lysine binding channel, and these interactions were absent in the GLP−**2a** complex. Other key features include the following: (1) the distal nitrogen of the

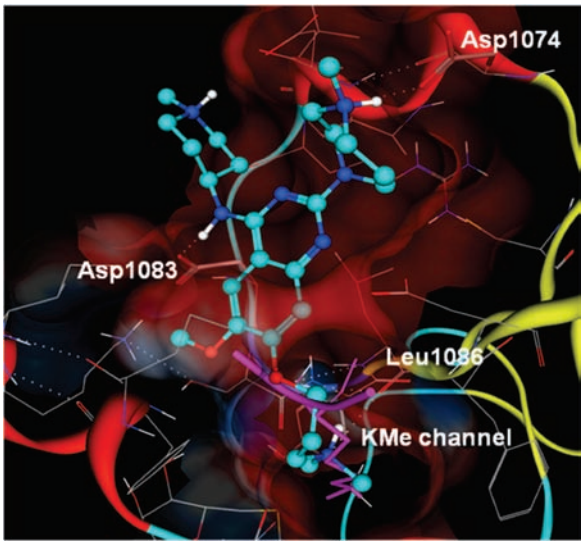

Figure 5. X-ray crystal structure of the G9a−**8** complex (PDB code 3K5K). Compound **8** is in light and dark blue. The superposed histone backbone trace and the methylated lysine side chain are in magenta.

homopiperazine interacts with Asp1074; (2) 4-amino group interacts with Asp1083; (3) the bulk of **8** occupies the histone peptide binding site. The inhibitor−enzyme interactions revealed by this high resolution cocrystal structure will enable future structure-based design of novel HMT inhibitors.

In conclusion, **8**, a potent and selective inhibitor of histone lysine methyltransferase G9a, was discovered via SAR exploration and structure-based design. The first X-ray crystal structure of G9a with a small molecule inhibitor was obtained. This high resolution cocrystal structure of the G9a−**8** complex validated our binding hypothesis and will enable structure-based design of novel inhibitors. **8** is a potentially valuable small molecule tool for the research community to investigate the biology of G9a and its roles in chromatin regulation.

Acknowledgment. We thank Dr. Yizhou Dong and Professor K. H. Lee for HRMS and HPLC support.

Supporting Information Available: Procedures and characterization data for all compounds; procedures for biochemical assays. This material is available free of charge via the Internet at http://pubs.acs.org.

References

(1) Bernstein, B. E.; Meissner, A.; Lander, E. S. The mammalian epigenome. *Cell* **2007**, *128*, 669–681.
(2) Gelato, K. A.; Fischle, W. Role of histone modifications in defining chromatin structure and function. *Biol. Chem.* **2008**, *389*, 353–363.
(3) Strahl, B. D.; Allis, C. D. The language of covalent histone modifications. *Nature* **2000**, *403*, 41–45.
(4) Jenuwein, T.; Allis, C. D. Translating the histone code. *Science* **2001**, *293*, 1074–1080.
(5) Esteller, M. Epigenetics in cancer. *N. Engl. J. Med.* **2008**, *358*, 1148–1159.
(6) Lyko, F.; Brown, R. DNA methyltransferase inhibitors and the development of epigenetic cancer therapies. *J. Natl. Cancer Inst.* **2005**, *97*, 1498–1506.
(7) Martin, C.; Zhang, Y. The diverse functions of histone lysine methylation. *Nat. Rev. Mol. Cell Biol.* **2005**, *6*, 838–849.
(8) Rea, S.; Eisenhaber, F.; O'Carroll, D.; Strahl, B. D.; Sun, Z. W.; Schmid, M.; Opravil, S.; Mechtler, K.; Ponting, C. P.; Allis, C. D.; Jenuwein, T. Regulation of chromatin structure by site-specific histone H3 methyltransferases. *Nature* **2000**, *406*, 593–599.
(9) Kouzarides, T. Chromatin modifications and their function. *Cell* **2007**, *128*, 693–705.
(10) Spannhoff, A.; Sippl, W.; Jung, M. Cancer treatment of the future: inhibitors of histone methyltransferases. *Int. J. Biochem. Cell Biol.* **2009**, *41*, 4–11.
(11) Fog, C. K.; Jensen, K. T.; Lund, A. H. Chromatin-modifying proteins in cancer. *APMIS* **2007**, *115*, 1060–1089.
(12) McGarvey, K. M.; Fahrner, J. A.; Greene, E.; Martens, J.; Jenuwein, T.; Baylin, S. B. Silenced tumor suppressor genes reactivated by DNA demethylation do not return to a fully euchromatic chromatin state. *Cancer Res.* **2006**, *66*, 3541–3549.
(13) Kondo, Y.; Shen, L.; Ahmed, S.; Boumber, Y.; Sekido, Y.; Haddad, B. R.; Issa, J. P. Downregulation of histone H3 lysine 9 methyltransferase G9a induces centrosome disruption and chromosome instability in cancer cells. *PLoS ONE* **2008**, *3*, No. e2037.
(14) Greiner, D.; Bonaldi, T.; Eskeland, R.; Roemer, E.; Imhof, A. Identification of a specific inhibitor of the histone methyltransferase SU(VAR)3-9. *Nat. Chem. Biol.* **2005**, *1*, 143–145.
(15) Kubicek, S.; O'Sullivan, R. J.; August, E. M.; Hickey, E. R.; Zhang, Q.; Teodoro, M. L.; Rea, S.; Mechtler, K.; Kowalski, J. A.; Homon, C. A.; Kelly, T. A.; Jenuwein, T. Reversal of H3K9me2 by a small-molecule inhibitor for the G9a histone methyltransferase. *Mol. Cell* **2007**, *25*, 473–481.
(16) Cole, P. A. Chemical probes for histone-modifying enzymes. *Nat. Chem. Biol.* **2008**, *4*, 590–597.
(17) Chang, Y.; Zhang, X.; Horton, J. R.; Upadhyay, A. K.; Spannhoff, A.; Liu, J.; Snyder, J. P.; Bedford, M. T.; Cheng, X. Structural basis for G9a-like protein lysine methyltransferase inhibition by BIX-01294. *Nat. Struct. Mol. Biol.* **2009**, *16*, 312–317.
(18) The G9a ThioGlo assay IC_{50} values in this paper are the average of at least duplicate assay runs with standard deviation (SD) within 1-fold unless noted otherwise. The G9a AlphaScreen IC_{50} values in this paper are the average of at least duplicate assay runs with standard error of the mean (SEM) $<35\%$. The observed potency difference for **2a** (BIX-01294) in our G9a ThioGlo and AlphaScreen assays (Table 1) versus the previously reported IC_{50} values (shown in Figure 1) is due to use of different assays.
(19) Collazo, E.; Couture, J. F.; Bulfer, S.; Trievel, R. C. A coupled fluorescent assay for histone methyltransferases. *Anal. Biochem.* **2005**, *342*, 86–92.
(20) Quinn, A. M.; Allali-Hassani, A.; Vedadi, M.; Simeonov, A. A chemiluminescence-based method for identification of histone lysine methyltransferase inhibitors. *Mol. BioSyst.*, submitted. G9a AlphaScreen assay protocol is included in Supporting Information.
(21) Min, J.; Allali-Hassani, A.; Nady, N.; Qi, C.; Ouyang, H.; Liu, Y.; MacKenzie, F.; Vedadi, M.; Arrowsmith, C. H. L3MBTL1 recognition of mono- and dimethylated histones. *Nat. Struct. Mol. Biol.* **2007**, *14*, 1229–1230.
(22) DSF graphs of **8** (UNC0224) and **2a** are included in Supporting Information.